Sequential Landfall of Tropical Cyclones in the United States: From Historical Records to Climate Projections

Dazhi Xi[1], Ning Lin[1]

[1]Department of Civil and Environmental Engineering, Princeton University

Corresponding author: Dazhi Xi (dxi@princeton.edu)

Keywords:

Tropical cyclones, Sequential landfall, Poisson-Gaussian model, Climate projection

Key Points:

- Time intervals between sequential landfalling TCs has decreased for most US regions, although the trend is not statistically significant.
- A climate downscaling projection indicates that intervals between sequential US landfalling TCs may significantly decrease in the future.
- The decreased intervals and increased chances of sequential landfalling TCs are mainly driven by increases in storm landfall frequency.

Abstract

In this study, we examine sequential landfalling tropical cyclones (TCs) along U.S. East and Gulf Coasts. We find that Florida and Louisiana are most prone to sequential landfall risk. The minimal time between sequential landfalling TC has decreased for most regions since 1979, although the trend is not statistically significant given limited data. A climate projection indicates a significant increase in sequential landfalls over the 21st century under the SSP5 8.5 scenario, with the chance of a location experiencing a less-than-10-day break between two TC impacts being doubled for most regions. The increases in sequential landfalls in the historical period and projected future climate are both related to increased landfall frequency, even though the storm season has been slightly expanding and may continue to expand. This study highlights a new type of TC hazard resulting from the temporal compounding of landfalls and urges the improvement of coastal resilience.

Plain Language Summary

Sequential landfalling tropical cyclones (TCs), which make landfall near a location within a short period of time, can be hazardous for coastal communities. Analyzing the historical records for the U.S. East and Gulf Coasts, we find that the states of Florida and Louisiana are most prone to sequential TC hazard, and this hazard has had an increasing potential for most coastal regions since 1979. Performing future projections of TCs under the effect of climate change, we find that the sequential TC hazard may increase even more significantly in the future. The increased sequential TC hazard in both the historical period and a projected future climate is related to the increased annual frequency of landfalling TCs. This study highlights a new type of TC hazard resulting from the temporal compounding of landfalling TCs and urges the improvement of coastal resilience, e.g., shortening the time scales for infrastructure recovery after TC landfalls.

1 Introduction

In 2020, 31 tropical cyclones (TCs) occurred in the North Atlantic. Besides the large number of TCs (tied with 2005 as the most since 1979), 18 TCs approached within 250 km of U.S. coastlines, the highest number since 1979. Eastern Louisiana, in particular, experienced sequential landfalls of three TCs. Tropical Storm Beta, Hurricane Delta, and Hurricane Zeta affected this region sequentially on September 20, October 9, and October 24, leading to losses of > $225 million, > $2.9 billion, and > $3.9 billion, respectively (Aon Benfiled 2020).

Sequential landfalling TCs (SLTs), defined as those that make landfall near a specific location within a short period of time, may be conceived as temporally compounding events (Zscheischler et al. 2020). SLTs are hazardous if the landfall interval is shorter than the time scale of recovery of coastal communities and ecosystems. For example, the time scale of power system recovery may be over two weeks; Ouyang et al. (2012) found that the power system in Harris County, Texas needed 16-17 days to fully recover after Hurricane Ike (2008) made landfall. Urban transportation systems may have similar recovery time scales; Chan and Schofer (2016) found that New York subway system restored 95% regular service two weeks after Hurricane Sandy (2012) made landfall. Also, TCs can weaken building structures and generate debris (Lin et al. 2010), which can take up to a year to clean up (Brandon et al. 2011) and weakened structures and scattered debris increase the chance for later storms to produce more damage (Minor 2005). Moreover, ecosystems are susceptible to SLTs, which can dramatically influence the concentration of nutrients (Paerl et al. 2001) or cause reductions in salinity (Switzer et al. 2016). Thus, a better understanding of SLTs supports the development of coastal resilience.

It is interesting from both scientific and social perspectives to ask if SLTs have been increasing and will increase in the future. Previous research has examined TC climatology features that are related to SLTs. Webster et al. (2005) found global increases of storm number since 1970s. Wang and Toumi (2021) found the fraction of storms entering coastal regions has an increased trend. Kossin et al. (2018) found the TC translation speed has decreased globally, and Hall and Kossin (2019) showed the stalling times of US landfalling TCs have increased. These results indicate increasing risks from TCs but did not directly address the trend of SLTs. For future projections, previous studies have focused on global to basin-scale changes of storm intensity and frequency. Most models project increased storm intensity and decreased frequency (Knutson et al. 2020) and some models project increased storm frequency (Emanuel 2013, Bhatia et al. 2018). Some models also project a slowdown of TC movement (Emanuel 2021) and increased TC landfall frequencies (Emanuel 2013, Emanuel 2021). Fewer studies have projected landfall hazards in the future (Marsooli et al. 2019, Emanuel 2017, Xu et al. 2020), and none of the climate projection studies has focused on SLTs.

In this study, we investigate SLTs in the coastal United States. We examine the time intervals between storm landfalls and impacts, as metrics describing SLTs, and their spatial and temporal variations. We also investigate how the climatology of these time intervals may change in the future, as simulated by a synthetic TC model downscaling six CMIP6 climate models. To explore the observed and simulated spatial and temporal variations of SLTs, we apply a Poisson-Gaussian model to connect TC landfall intervals to TC landfall frequency and seasonality.

2 Data and Method

To study the historical climatology of SLTs in the coastal United States, we used TC observations from the International Best Track Archive for Climate Stewardship (IBTrACS). IBTrACS provides six-hourly TC locations and intensities. We used data from 1979 (the satellite era) to avoid the influence of missing records in earlier decades (Moon et al. 2018).

To study climate change effect, we applied synthetic TCs generated with a statistical-deterministic TC model (Emanuel 2008, Emanuel 2021). The synthetic storms were generated under the environments of the NCAR/NCEP reanalysis and each of six CMIP6 climate models (CanESM5, CNRM-CM6-1, GFDL-CM-4, EC-Earth3, IPSL-CM6A-LR, MIROC6) for control (1984-2005) and Shared Socioeconomic Pathway 5 8.5 scenarios (SSP5 8.5; 2070-2100). 4400 and 6200 storms were generated from each climate model for control and SSP5 8.5 scenarios, respectively, and 5018 storms were generated from the reanalysis in the control period.

We divided the U.S. East and Gulf coastlines into eight regions, namely Texas, Louisiana, Mississippi-Alabama, West Florida, East Florida, Georgia, South Carolina, and North Carolina (regions in higher latitudes have been seldomly affected by SLTs and thus are not investigated in this study). We also specifically examine the East Louisiana region (90.59° W to 89.29° W) as it was hit by SLTs in 2020. To focus on SLTs that are spatially close enough to cause compound impacts, we divided the coastlines into 186 mileposts with 100-km spacing in Mexico and 50-km spacing in the US (detailed in Jing and Lin, 2020) and analyzed SLTs for each milepost. We selected all storms in IBTrACS and synthetic storm simulations that approached within 250 km of a milepost (following Jing and Lin, 2020) and defined the landfall time as when the storm first entered the 250-km circle centered on the milepost. We computed the landfall intervals between storms for each milepost and defined the minimum interval over a year and across all mileposts in each defined coastal region to be the minimal landfall interval (MLI) in the year for the region. We further defined the storm impact duration (SID) for a milepost as the duration when the storm was within 250 km of the milepost, and we calculated the minimal impact interval (MII), the minimum over a year and across the mileposts for the region of the time interval between the end of the impact of the first storm and the start of the impact of the second storm. Annual landfall frequencies for each region are also calculated.

We considered storms that reach tropical storm intensity (>17.5 m/s) at landfall in the historical analysis. For synthetic analysis with larger samples, we examined MLI and MII also for hurricanes (>32.5 m/s at landfall). We estimated the probability distribution and return period for MLI and MII in the control simulations and climate-model projections. The climate projections of MLI and MII were bias-corrected. We bias-corrected the future projection of storm frequency and cumulative density functions (CDFs) of MLI and MII in each model by comparing the climate-model and reanalysis-based estimations for the control period. The storm frequency was bias-corrected through a multiplicative factor, and CDFs of MLI and MII were bias-corrected through quantile-quantile-mapping. Besides the MLI and MII distributions for each of the six climate models, we also calculated the weighted average of the six models, by assigning weights to the models based on the mean square error of the model-simulated CDFs of MLI and MII for the control period compared to reanalysis-based simulations. Marsooli et al. (2019) applied similar methods to perform bias correction and model combination for storm surge projections.

To understand the connections between MLI and landfall frequency and seasonality, we propose a Poisson-Gaussian landfall model. The model assumes storm arrivals in a region to form a nonstationary Poisson process. The Poisson rate of storm landfall is modulated by interannual and seasonal variations, which can be described as

$$\nu(t,s) = \lambda(t)S(s) \tag{1}$$

where $\lambda(t)$, the interannual variation, is the landfall frequency in year *t*, and $S(s)$, the seasonal variation, is the likelihood of landfall occurrence on day *s* relative to the likelihood of occurrence during the season. We model the seasonality with a Gaussian function,

$$S(s) = \frac{1}{\sigma\sqrt{2\pi}} e^{-\frac{1}{2}(\frac{s-\mu}{\sigma})^2} \tag{2}$$

where $\boldsymbol{\mu}$ is the mean landfall day during the year and $\boldsymbol{\sigma}$ is the standard deviation of the landfall day. While $\boldsymbol{\mu}$ represents the seasonal peak, $\boldsymbol{\sigma}$ represents the spread of the season. In this model, MLI depends solely on $\boldsymbol{\sigma}$ and λ, as they together determine the number of storms within a time period, while $\boldsymbol{\mu}$ has no influence on MLI as it only shifts the landfall day. We performed Monte Carlo simulations of storm landfalls for various $\boldsymbol{\sigma}$ and λ to examine the theoretical connection between MLI and these parameters.

Based on this landfall model, we investigated the change of MLI by investigating the changes of λ and $\boldsymbol{\sigma}$ in historical observations and climate simulations. To study how these parameters have changed in the historical period, we divided the historical period (1979-2019) into two periods (1979-1999 and 2000-2019) and fitted the model for each period. To study how these parameters may change from the control to the future climate, we fitted the model for the control and future periods for each climate model. We used the method of maximum likelihood for model fitting. We performed Monte Carlo simulations of TC landfall using the model fitted by the historical observation to validate the model.

The Poisson-Gaussian model assumes storms are conditionally independent (given the environmental condition), and so does the synthetic storm modeling, as feedbacks of storms to the environment is not captured in the one-way coupling system. Physical interactions between storms are possible but rare (Hoover 1961, Brand 1970, Xu et al. 2013, Schenkel 2016). Also, previous research has examined the independence assumption on storm genesis and landfalls and found that the Poisson distribution generally fits the observations well (e.g., Rumpf et al. 2009, Lin et al. 2012, Wahiduzzaman et al. 2021).

3 Historical Record of SLTs

We first use East Louisiana as an example to study the historical variation of the annual landfall frequency, mean SID, and MLI. Figure 1 (a)-(d) shows that, for East Louisiana, the landfall frequency has increased by 0.0167±0.0156 storms/year since 1979. SID has increased by 0.016±0.011 days/year since 1979. Also, MLI has decreased (-0.909±0.508 days/year) since 1979, implying that the chance of SLTs has increased. The increasing trends of the landfall frequency and mean SID pass the Mann-Kendall significance test (95% confidence level), but the trend of MLI cannot pass the test, possibly due to data limitations (only data in years with at least two landfalling storms at a milepost are used to calculate MLI). The probability distribution of yearly MLI is fitted with a Generalized Pareto Distribution (GPD) (Fig.1d). The shape parameter of the fitted GPD is negative, implying that the GPD has a light tail and the yearly MLI is unlikely to take values much larger than the mean.

We extended the above analysis to the other coastal regions (Fig. 1(e)-(h)). Except for Texas, all the other coastal regions show a slight but statistically significant increase of landfalling frequency since 1979 (up to 0.04±0.0182 storms/year). Significant increases of SID are observed for all the coastal regions, with the maximum increase occurring in Louisiana (0.0286±0.0105 days/year). The observed increase in SID is consistent with the finding of Hall and Kossin (2019). MLI decreases for most regions, except West Florida and Mississippi-Alabama, by up to 0.94±0.75 days/year (South Carolina). Although the trend cannot pass the Mann-Kendall test due to data limitation, the increased landfall frequency indicates increased potential for short MLI (see discussion with the theoretical modeling below). The decrease in MLI and increase in SID implies a decrease of MII (not shown) and thus an increase of impact from SLTs for most coastal areas. We also fit GPD to MLI for each region; Fig. 1(h) shows the scale of the fitted GPD. Small value of the scale indicates the region is more likely to experience short MLI. The lowest values of scale are found in East Florida (24.41), West Florida (32.02), and Louisiana (37.79), meaning that these locations are most prone to the threat of SLTs. Shape parameters (not shown) for all regions are negative except for Florida, implying that MLI is unlikely to take values much larger than the mean in most regions.

To better understand the variation of MLI, we investigate the connection between MLI and TC climatology features. Figure 2(a) shows the relationship between MLI and the annual landfall frequency in the historical record. Smaller MLI is associated with larger landfall frequency. Linear fitting of mean MLI to annual landfall frequency indicates that one more landfall on average causes a 7.15±2.4-day shortening of MLI. Figure 2(b) shows the relationship between the fitted $\boldsymbol{\lambda}$ (annual frequency averaged over each period) and $\boldsymbol{\sigma}$ (seasonality variation averaged over each period) in the historical record, and how they jointly influence MLI. We find that $\boldsymbol{\lambda}$ and $\boldsymbol{\sigma}$ are positively correlated, implying that as the storm frequency increases (Fig. 1(e)), storm season has also been slightly expanding (i.e., seasonal distribution being slightly flattened). Figure 2(b) also shows that lower MLI is associated with smaller $\boldsymbol{\sigma}$ and larger $\boldsymbol{\lambda}$ although the pattern appears unclearly due to data limitations. Thus, we perform idealized simulations using the Poisson-Gaussian model; Figure 2(c) shows the expectation of MLI (E(T)) in the $\boldsymbol{\lambda}-\boldsymbol{\sigma}$ space. The theoretical results show that given σ, the larger the λ, the lower the MLI and given λ, the smaller the σ, the lower the MLI. MLI is shortened by about 6-8 days per increase of a landfall, consistent with the empirical sensitivity. The Poisson-Gaussian model is evaluated with the observation (Figure 2(d)). The model captures the relationship between MLI and parameters $\boldsymbol{\lambda}$ and $\boldsymbol{\sigma}$ well. All observations are covered by the 25-th to 75-th percentiles of the Monte Carlo simulations. The small discrepancies of simulations and observations are related to the model assumption of storm independency and statistical uncertainties. The result indicates that MLI has a decreasing potential over the historical period mainly because the storm landfall frequency has increased. Although the storm season has been slightly expanding (i.e., TC activity in the off-peak season has increased relatively more than in the peak season), the increase of TC activity in the peak season is still significant and likely responsible for the decrease of MLI.

4 Climate Projection of SLTs

In this section we use the synthetic storm dataset to examine SLTs under climate change. Figure 3 examines the CDF of MLI. We find that the probability for short TC-MLI (MLI between TCs; Figs. 3a–3h) increases from the control to the future climate (e.g., in Louisiana the probability of MLI < 20 days increases from 0.49 to 0.65), while the predicted degree of increase varies among climate models. The probability for short hurricane-MLI (MLI between hurricanes; Figs. 3i-3p) also increases (e.g., in Louisiana the probability of hurricane-MLI < 20 days increases from 0.52 to 0.61), and the changes in the Gulf Coast regions and Florida are larger than those in East Coast regions. The overall chance of the hurricane-MLI being smaller than 20 days for the Gulf Coast (Texas to West Florida) increases from 0.46 to 0.59 and for East Coast (East Florida to North Carolina) increases from 0.46 to 0.56 (not shown). All changes pass the two-sample

Kolmogorov-Smirnov test on differences in distributions (with 5% significance level) and are hence statistically significant.

To assess overall sequential landfall risk, we combine MLI, SID, and multi-landfall frequency to compute return period of MII (Figure 4). The change in MII is significant, which is dominated by the change in MLI and landfall frequency rather than SID (not shown). For example, the return period of a 10-day TC-MII would decrease by about half for most regions from the control to future climate (e.g., in Louisiana the return period decreases from 15 years to 8 years). We found more significant increase of the chance of experiencing a short hurricane-MII (break between hurricane impacts). In Louisiana the return period of a 20-day hurricane-MII would decrease from 35 to 4 years. For the Gulf Coast (Texas to West Florida) the return period of a 20-day hurricane-MII would decrease from 12 to one year, and for the East Coast (East Florida to North Carolina) it will decrease from 25 to two years (not shown).

To better understand the change of SLTs in the future, we examine the change of annual landfall frequency $\boldsymbol{\lambda}$ and seasonality $\boldsymbol{\sigma}$ in the control and future climate simulations from the six climate models. We find that the averages of both $\boldsymbol{\lambda}$ and $\boldsymbol{\sigma}$ increase in the future. The increase in average $\boldsymbol{\lambda}$ from the control to the future climate ranges from 2.38 to 6.31 storms across the regions while the increase in average $\boldsymbol{\sigma}$ ranges from 3.69 to 4.87 days. The increase in $\boldsymbol{\lambda}$ is a composite result of increased basin-wide genesis frequency and northward expansion of track density (Emanuel 2021). The projected change in $\boldsymbol{\lambda}$ over the 21th century is beyond the historical variation from the period of 1979-1999 to the period of 2000-2019 (increase by up to 0.9 storms) while the increase in $\boldsymbol{\sigma}$ is within the historical variation (increase by up to 9.6 days). According to the Poisson-Gaussian model (Fig. 2c), such changes in storm frequency and seasonality lead to the significant decrease of MLI (e.g., in Louisiana expected MLI decreases from around 17 days to 6 days; Fig. 3) and MII (Fig. 4), resulting from increased storm activity in the peak season.

5 Conclusions

This study examines various climatological features of SLTs using observation and climate model projections for U.S. East and Gulf Coasts. We describe SLTs with storm landfall interval (MLI), impact duration (SID), and impact interval (MII). We find East Florida, West Florida, and Louisiana are most prone to sequential SLTs risk. Except for Texas, the landfall frequency and annual mean SID have significantly increased since 1979, with the largest increase in landfall frequency found in Mississippi-Alabama (+0.04±0.0182 storms/year) and the largest increase in SID found in Louisiana (+0.0286±0.0105 days/year). MLI decreases for most regions, except West Florida and Mississippi-Alabama, by up to 0.94±0.75 days/year (South Carolina). Although the trend is not statistically significant due to data limitation, the increase of landfalling storms indicate increased potential for short MLI for most regions in the U.S. Coasts. The decreasing potential of MLI and increases in landfall frequency and SID indicate decreased MII and thus an increased impact from SLTs for most coastal areas. Applying a Poisson-

Gaussian model, we found the decrease of MLI is consistent with the increase of annual landfall frequency, although the storm season has also been slightly expanding. Previous findings of more storms (Webster et al. 2005, Wang and Toumi 2021) and longer storm stalling time (Hall and Kossin 2019) and our results of increased likelihood of temporally compounding storms consistently indicate an increased TC threat along the U.S. coastlines over the past decades.

Climate projections using a synthetic storm model indicate SLTs will significantly increase under the SSP5 8.5 scenario, especially for the Gulf Coast. The return period of a 10-day MII between TCs would decrease by about half for most coastal regions over the 21^{st} century (e.g., in Louisiana from 15 years to 8 years). The chance of experiencing a short MII between hurricanes would increase more significantly (e.g., in Louisiana the return period of a 20-day hurricane-MII would decrease from 35 years to 4 years). This large increase in SLTs is consistent with the projected significant increase of annual landfall frequency in the model (increased by 2.38-6.31 storms on average over the 21^{st} century for US coast) although the storm season is projected to be slightly expanding. Previous research has projected a global slowdown of storm translation speed (Emanuel 2021) and more landfalling storms in the future (Emanuel 2013, Emanuel 2021). Consistent with the previous findings, this study shows explicitly that the time intervals between storm impacts may significantly decrease in the future.

This study highlights a new type of TC hazard resulting from temporally compounding landfalls while previous studies focus on single-storm hazards such as surge (Marsooli et al. 2019), rainfall (Emanuel 2017), and compound flooding (Gori et al. 2020). Previous findings on intensified single-storm hazards calls for improvement of coastal reliability while this study on increased SLTs urges the improvement of coastal resilience. For example, the power system in Texas requires around 17 days to fully recover after hurricane landfall (Ouyang et al. 2012). For Texas, hurricane-MII being less than 17 days is a 40-year event in the current climate but would be a less-than-10-year event in the future (Figure 4i). To be prepared for potentially more frequent SLTs in the future, the recovery time of power grids and other infrastructure systems may need to be shortened along U.S. coastlines.

This study used a specific synthetic storm model to investigate SLTs in the future climate. This storm model predicts increased TC frequencies (Emanuel 2013, 2021) while large uncertainties still exist on how TC frequency will change in the future (Knutson et al. 2020). This study underlines again the importance of accurately projecting TC frequency, which greatly influences the estimation of SLTs and other TC hazards (Marsooli et al. 2019). It is important for future studies to use other methods, including regional (Wright et al. 2015) and global climate models that can explicitly simulate intense TCs (e.g., Bhatia et al. 2018), to validate the change of SLTs in the future found in this study.

Data Availability Statement

The analysis results and data from this study are deposited to the NSF DesignSafe-CI and can be accessed online (https://www.designsafe-ci.org/data/browser/projects/7419478767301693931-242ac117-0001-012/). The hurricane dataset IBTrACS can be accessed from the National Climatic Data Center (https://www.ncdc.noaa.gov/ibtracs/). The original synthetic tropical cyclone datasets used in this study are freely available from Kerry Emanuel for research purposes. For the details and availability of the synthetic datasets, please refer to Emanuel (2021) (DOI: https://doi.org/10.1175/JCLI-D-20-0367.1)

Acknowledgments

This material is based upon work supported by the National Science Foundation (NSF Grants 1854993 and 1652448). All opinions expressed in this paper are the authors' and do not necessarily reflect the policies and views of NSF. The authors thank Kerry Emanuel (MIT) for providing us with the synthetic storm datasets and constructive comments. The first author also thanks Tianqi Cui (JHU) for useful discussions about the statistical analysis.

References

Aon Benfield. 2021. "Global Catastrophe Recap – October 2020" (PDF). p. 4.

Bhatia, K., Vecchi, G., Murakami, H., Underwood, S., & Kossin, J. (2018). Projected response of tropical cyclone intensity and intensification in a global climate model. *Journal of Climate*, *31*(20), 8281–8303. https://doi.org/10.1175/JCLI-D-17-0898.1

Brand, S. (1970), Interaction of binary tropical cyclones of the western North Pacific Ocean, *J. Appl. Meteor*., 9, 433-441.

Brandon, D. L., Medina, V. F., & Morrow, A. B. (2011). A case history study of the recycling efforts from the United States Army Corps of Engineers Hurricane Katrina debris removal mission in Mississippi. *Advances in Civil Engineering*, *2011*(3). https://doi.org/10.1155/2011/526256

Chan, R., & Schofer, J. L. (2016). Measuring Transportation System Resilience: Response of Rail Transit to Weather Disruptions. *Natural Hazards Review*, *17*(1), 05015004. https://doi.org/10.1061/(asce)nh.1527-6996.0000200

Emanuel, K. (2017). Assessing the present and future probability of Hurricane Harvey's rainfall. *Proceedings of the National Academy of Sciences of the United States of America*, *114*(48), 12681–12684. https://doi.org/10.1073/pnas.1716222114

Emanuel, K. (2006). Climate and tropical cyclone activity: A new model downscaling approach. *Journal of Climate*, *19*(19), 4797–4802. https://doi.org/10.1175/JCLI3908.1

Emanuel, K. (2021). Response of global tropical cyclone activity to increasing CO2: Results from downscaling CMIP6 models. *Journal of Climate*, *34*(1), 57–70. https://doi.org/10.1175/JCLI-D-20-0367.1

Hall, T. M., & Kossin, J. P. (2019). Hurricane stalling along the North American coast and implications for rainfall. *Npj Climate and Atmospheric Science*, *2*(1), 1–9. https://doi.org/10.1038/s41612-019-0074-8

HOOVER, E. W. (1961). Relative Motion of Hurricane Pairs. *Monthly Weather Review*, *89*(7), 251–255. https://doi.org/10.1175/1520-0493(1961)089<0251:rmohp>2.0.co;2

Jing, R., & Lin, N. (2020). An Environment-Dependent Probabilistic Tropical Cyclone Model. *Journal of Advances in Modeling Earth Systems*, *12*(3), 1–18. https://doi.org/10.1029/2019MS001975

Knutson, T. R., McBride, J. L., Chan, J., Emanuel, K., Holland, G., Landsea, C., et al. (2010). Tropical cyclones and climate change. *Nature Geoscience*, *3*(3), 157–163. https://doi.org/10.1038/ngeo779

Knutson, T. R., J. J. Sirutis, M. Zhao, R. E. Tuleya, M. Bender, G. A. Vecchi, G. Villarini, and D. Chavas, 2015: Global projections of intense tropical cyclone activity for the late twenty-first century from dynamical downscaling of CMIP5/RCP4.5 scenarios. J. Climate, 28, 7203–7224, https://doi.org/10.1175/JCLI-D-15-0129.1.

Knutson, T., Camargo, S. J., Chan, J.C., Emanuel, K., Ho, C. H., Kossin, J., Mohapatra, M., Satoh, M., Sugi, M., Walsh, K. and Wu, L., 2020. Tropical cyclones and climate change assessment: Part II: Projected response to anthropogenic warming. Bulletin of the American Meteorological Society, 101(3), pp. E303-E322.

Kossin, J. P. (2018). A global slowdown of tropical-cyclone translation speed. *Nature*, *558*(7708), 104–107. https://doi.org/10.1038/s41586-018-0158-3

Lee, C. Y., Camargo, S. J., Sobel, A. H., & Tippett, M. K. (2020). Statistical-Dynamical downscaling projections of tropical cyclone activity in a warming climate: Two diverging genesis scenarios. *Journal of Climate*, *33*(11), 4815–4834. https://doi.org/10.1175/JCLI-D-19-0452.1

Lin, N., E. Vanmarcke, and S. C. Yau (2010). Windborne debris risk analysis – Part II. Application to structural vulnerability modeling. Wind. Struct. 13(2): 207-220.

Lin, N., Emanuel, K., Oppenheimer, M., & Vanmarcke, E. (2012). Physically based assessment of hurricane surge threat under climate change. *Nature Climate Change*, *2*(6), 462–467. https://doi.org/10.1038/nclimate1389

Marsooli, R., Lin, N., Emanuel, K., & Feng, K. (2019). Climate change exacerbates hurricane flood hazards along US Atlantic and Gulf Coasts in spatially varying patterns. *Nature Communications*, *10*(1), 1–9. https://doi.org/10.1038/s41467-019-11755-z

Minor, J. E. (2005). Lessons Learned from Failures of the Building Envelope in Windstorms. *Journal of Architectural Engineering*, *11*(1), 10–13. https://doi.org/10.1061/(asce)1076-0431(2005)11:1(10)

Moon, I.-J., Kim, S.-H., & Chan, J. C. L. (2019). Climate change and tropical cyclone trend. Nature, 570(7759), E3–E5. https://doi.org/ 10.1038/s41586-019-1222-3

Ouyang, M., Dueñas-Osorio, L., & Min, X. (2012). A three-stage resilience analysis framework for urban infrastructure systems. *Structural Safety*, *36–37*, 23–31. https://doi.org/10.1016/j.strusafe.2011.12.004

Paerl, H. W., Bales, J. D., Ausley, L. W., Buzzelli, C. P., Crowder, L. B., Eby, L. A., et al. (2001). Ecosystem impacts of three sequential hurricanes (Dennis, Floyd, and Irene) on the United States' largest lagoonal estuary, Pamlico Sound, NC. *Proceedings of the National Academy of Sciences of the United States of America*, *98*(10), 5655–5660. https://doi.org/10.1073/pnas.101097398

Schenkel, B. A. (2016). A climatology of multiple tropical cyclone events. *Journal of Climate*, *29*(13), 4861–4883. https://doi.org/10.1175/JCLI-D-15-0048.1

Switzer, T. S., Winner, B. L., Dunham, N. M., Whittington, J. A., & Thomas, M. (2006). Influence of sequential hurricanes on nekton communities in a Southeast Florida estuary: Short-term effects in the context of historical variations in freshwater inflow. *Estuaries and Coasts*, *29*(6), 1011–1018. https://doi.org/10.1007/bf02798663

Wahiduzzaman, M., Yeasmin, A., Luo, J. J., Quadir, D. A., Van Amstel, A., Cheung, K., & Yuan, C. (2021). Markov Chain Monte Carlo simulation and regression approach guided by El Niño–Southern Oscillation to model the tropical cyclone occurrence over the Bay of Bengal. Climate Dynamics, 56(9), 2693-2713.

Wang, S., & Toumi, R. (2021). Recent migration of tropical cyclones toward coasts. *Science*, *371*(6528), 514–517. https://doi.org/10.1126/science.abb9038

Wright, D. B., Knutson, T. R., & Smith, J. A., 2015. Regional climate model projections of rainfall from U.S. landfalling tropical cyclones

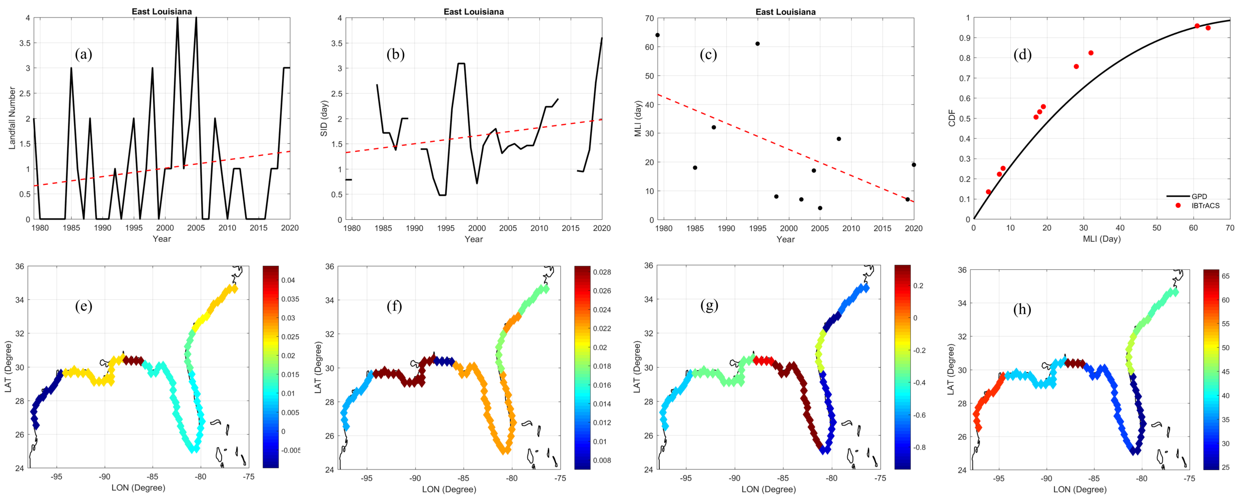

Figure 1. Analysis of historical SLTs from 1979-2020. Upper panels: East Louisiana. (a). Annual landfall frequency, (b). Annual mean storm impact duration (SID), and (c). Annual minimal landfall interval (MLI); for (a), (b), and (c), the red line indicates the trend from 1979. (d). CDF of MLI from the data (red dots) and GPD fit (black curve) using data from 1979-2020. Bottom panels: U.S. East and Gulf coasts. Annual change ($year^{-1}$) of (e). landfall frequency, (f). mean SID, and (g). MLI. (h). Scale of fitted GPD of MLI of 1979-2020.

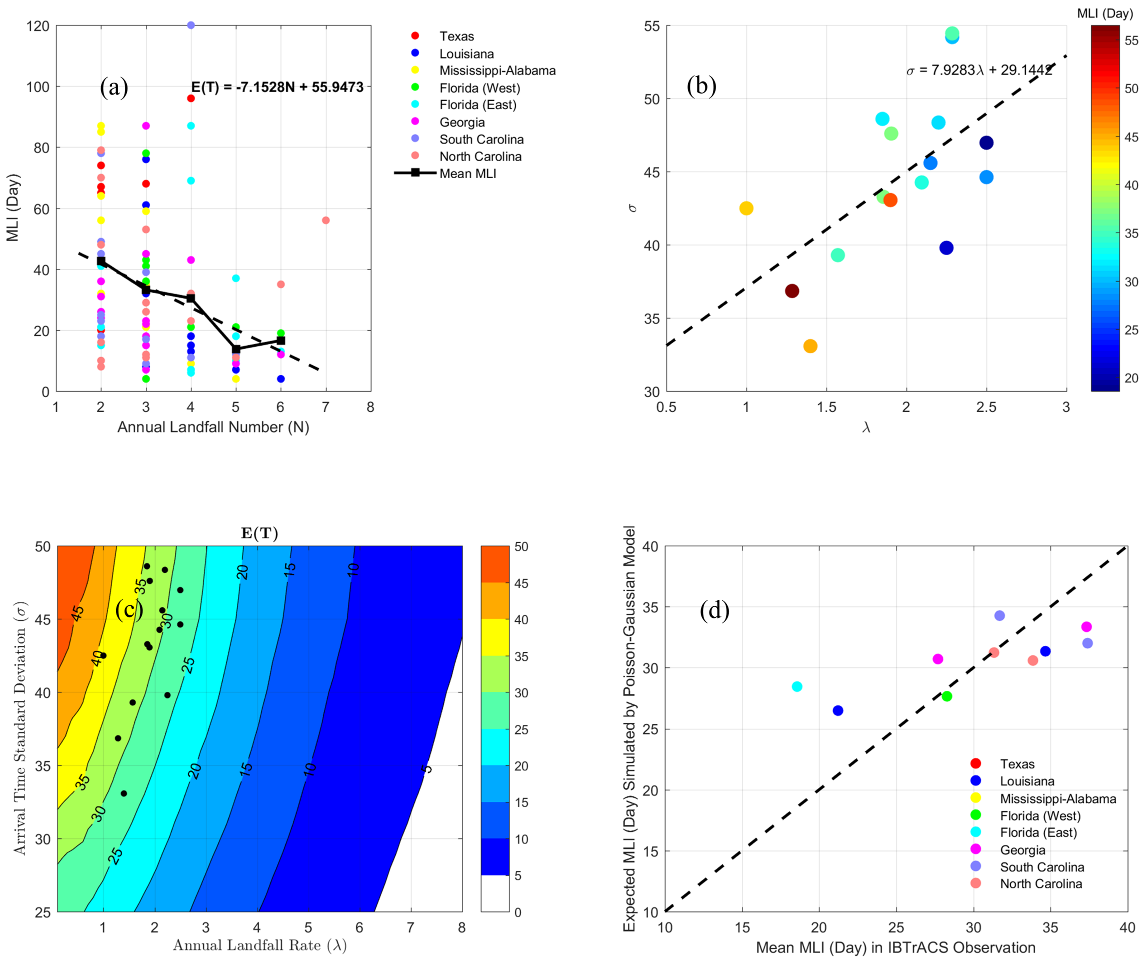

Figure 2. Analysis of the relationship between minimal landfall interval (MLI) and TC climatology features. (a) Observed relationship between MLI and annual landfall frequency. (b) Observed relationship between landfall frequency, λ, and standard deviation of the landfall day, σ. λ and σ are fitted for each of the two periods (1979-1999 and 2000-2019). (c) Expectation of MLI in the λ and $\boldsymbol{\sigma}$ space in the Poisson-Gaussian model; black dots are the observed λ and σ as in (b). (d). Comparison of simulated expectation and observed mean of MLI; only locations with more than three years of records of multi-storm landfalls are shown.

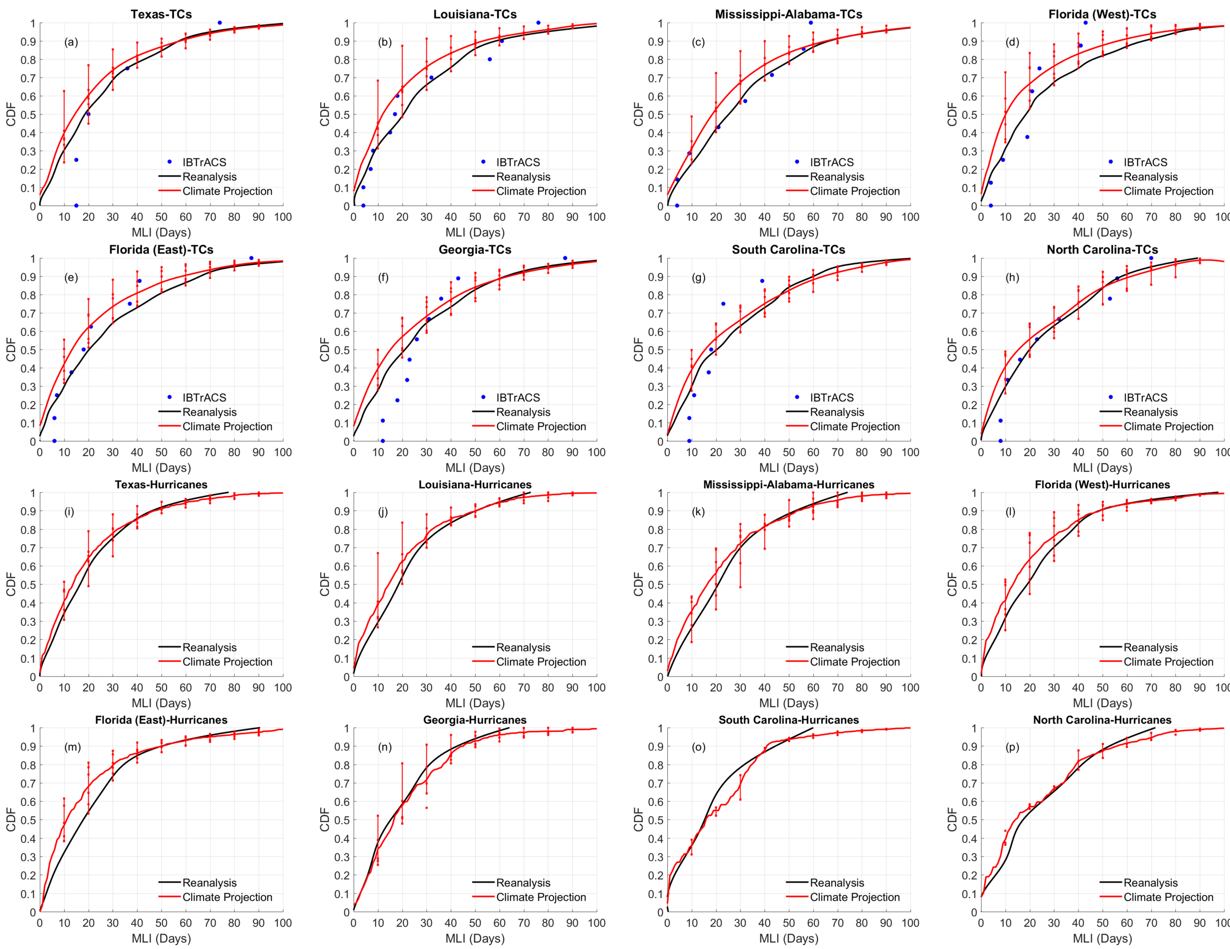

Figure 3. CDF of minimal landfall interval between TCs (TC-MLI) in (a) Texas, (b) Louisiana, (c) Mississippi-Alabama, (d) West Florida, (e) East Florida, (f) Georgia, (g) South Carolina, and (h) North Carolina. (i)-(p) are same as (a)-(h), but for hurricanes (hurricane-MLI). The CDF is calculated based on data in years when at least two TCs (or hurricanes) make landfall at a milepost in the region. Blue dots show observations (for TCs only), black curve shows the reanalysis-based simulation for the historical period, red curve shows the weighted average projection for the future climate, and the spread of the six climate models is shown as error bars. Bias-correction based on the reanalysis simulation is applied for the climate projections. (For North Carolina, three of six climate models (CanESM5, CNRM-CM6-1, IPSL-CM6A-LR) cannot predict SLTs for hurricanes in the historical period due to limited number of intense storms in historical simulations, so we omit the SSP5 8.5 simulations from these climate models for this location.)

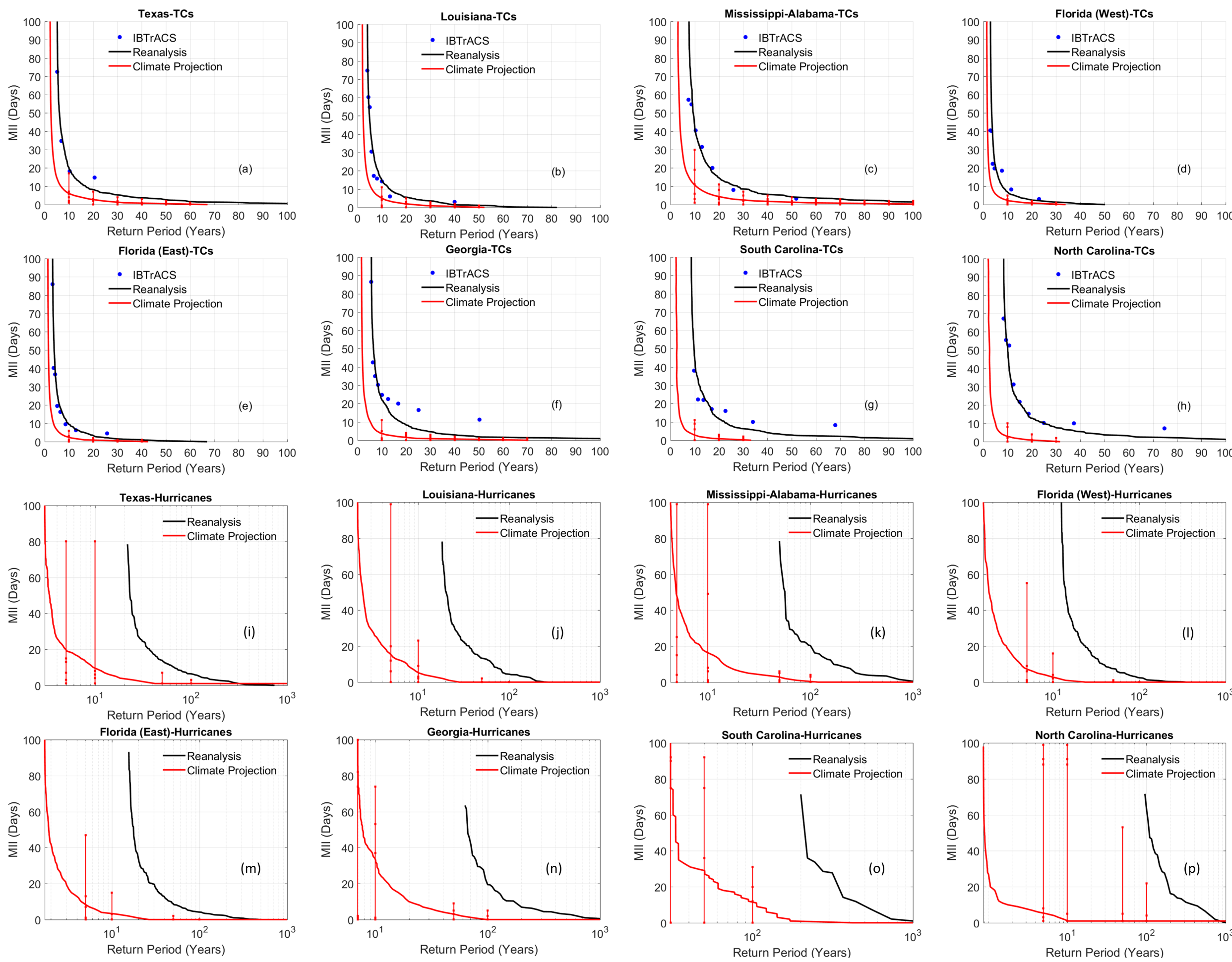

Figure 4. Same as Fig. 3, but for return period of minimal impact interval (MII).